The theory of cosmic ray acceleration and transport I. Key observations and electromagnetic acceleration processes

Reinhard Schlickeiser, Ruhr University Bochum, Germany

August 2018

Topics:

1. Introduction
2. Fundamental cosmic ray astrophysics
3. Basic kinetic equations
4. Cosmic particle distribution functions
5. In-situ observations
6. Decoupled dynamics
7. Summary lecture 1

Literature:

Cosmic ray astrophysics, RS, 2002, Springer, Berlin

Cosmic ray transport in astrophysical plasmas, RS, 2015, Phys. of Plasmas 22, 091502

1. Introduction

The detection of nonthermal radiation from many astrophysical objects requires the acceleration of charged particles to relativistic energies in these plasma systems. The acceleration mechanisms, whatever they may be, are remarkably efficient, converting a major fraction of the total energy into fast particles.

The principal limitation on particle acceleration theories has been the realisation (e.g. Parker (1976)) that the universe is not filled with a perfect vacuum, but rather is pervaded everywhere by tenous ionized gases with high electrical conductivity quite able to short circuit any large-scale electric fields that occur under ordinary circumstances. But electric fields are needed for electromagnetic particle acceleration.

Apart from unipolar inductor sources like pulsars and the electric field in perpendicular collisionless shock waves, the large electrical conductivity of most space plasmas prevents to sustain stationary and steady large-scale electric fields. Electric fields in space plasmas then only appear as (i) transient phenomena (as in magnetic reconnection situations), or as (ii) fluctuating fields (plasma turbulence) in magnetized gases

$$\vec{E} = \vec{0} + \ \delta \vec{E} \ , \vec{B} = \vec{B}_0 + \ \delta \vec{B} \tag{1}$$

with vanishing ensemble averages $< \delta \vec{E} >= 0$ and $< \delta \vec{B} >= 0$.

As a consequence, five basic types of electromagnetic particle acceleration processes in space plasmas have been considered in the literature:

(1) stochastic acceleration by particle interactions with plasma fluctuations,

(2) (diffusive) shock acceleration,

(3) focused acceleration in nonuniform magnetic fields,

(4) conversion of bulk motion to relativistic particles,

(5) acceleration by turbulent magnetic reconnection.

The most prominent energetic charged particle component in space are cosmic rays (CRs=charged particles with energies above 1 MeV) discovered first by Viktor Hess in 1912. Besides CR particles the electromagnetic acceleration theory can also be applied to suprathermal ions, electrons and dust particles.

As I will argue in Sect. 2 our current observational knowledge of cosmic rays strongly favours an electromagnetic CR acceleration process. For the processes (1)-(5) this requires a detailed understanding of the electromagnetic fluctuations in space.

Because of the large sizes of astrophysical systems the fluctuations are descibed by real wave vectors ($\vec{k}$) and complex frequencies $\omega(\vec{k}) = \omega_R(\vec{k}) + \imath\Gamma(\vec{k})$, implying for the space- and time-dependence of e.g. magnetic fluctuations the superpositions of

$$\delta\vec{B}(\vec{x},t) \propto \exp[\imath(\vec{k}\cdot\vec{x} - \omega_R t) + \Gamma t] \tag{2}$$

One distinguishes between

- **non-collective** fluctuations with no dispersion relation $\omega = \omega(\vec{k})$
- **collective** modes with a fixed dispersion relation $\omega = \omega(\vec{k})$, e.g. electromagnetic waves in vacuum $\omega_R^2 = c^2k^2$ and $\Gamma = 0$,

and regarding the real (ω_R) and imaginary (Γ) part of the frequency

- **weakly damped/amplified wave-like** fluctuations with $|\Gamma| \ll |\omega_R|$
- **weakly propagating** fluctuations with $|\omega_R| \ll |\Gamma|$, including **aperiodic** fluctuations with $\omega_R = 0$. Aperiodic modes fluctuate only in space, do not propagate as $\omega_R = 0$, but permanently grow or decrease in time depending on the sign of Γ.

In-situ plasma turbulence observations: the interplanetary medium is filled with aperiodic fluctuations in the form of mirror, firehose and ordinary mode oscillations, so that there is no doubt that they exist in nature!

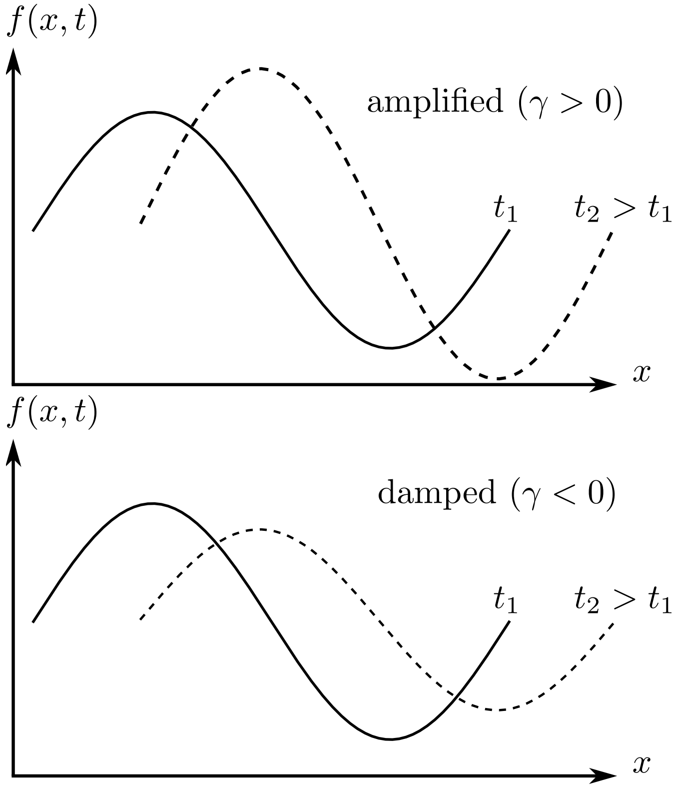

Figure 1: Sketch of weakly amplified ($\gamma > 0$, top) and weakly damped ($\gamma < 0$, bottom) monochromatic plasma wave ($\omega_R \gg |\gamma|$).

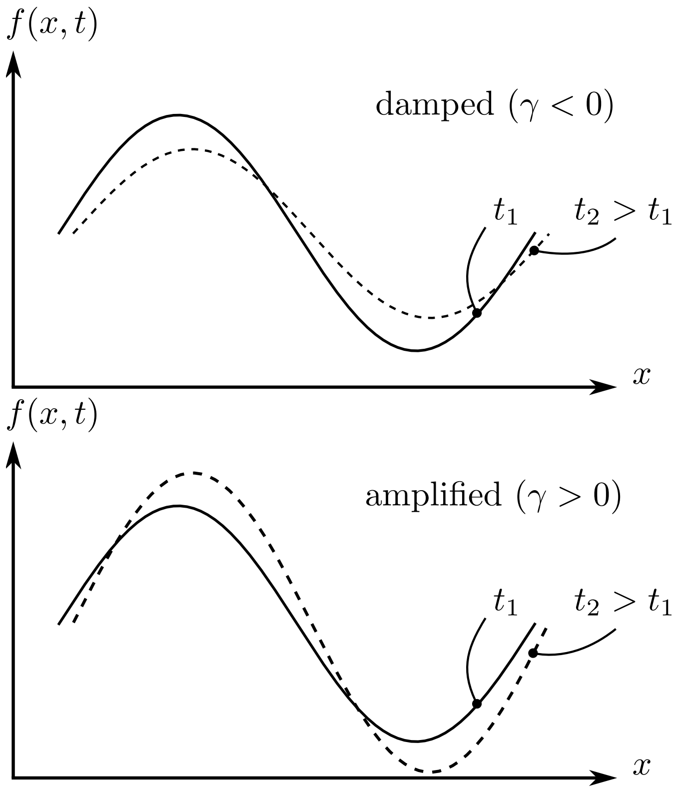

Figure 2: Sketch of weakly propagating damped ($\gamma < 0$, top) and weakly propagating amplified ($\gamma < 0$, bottom) monochromatic fluctuation ($\omega_R \ll |\gamma|$).

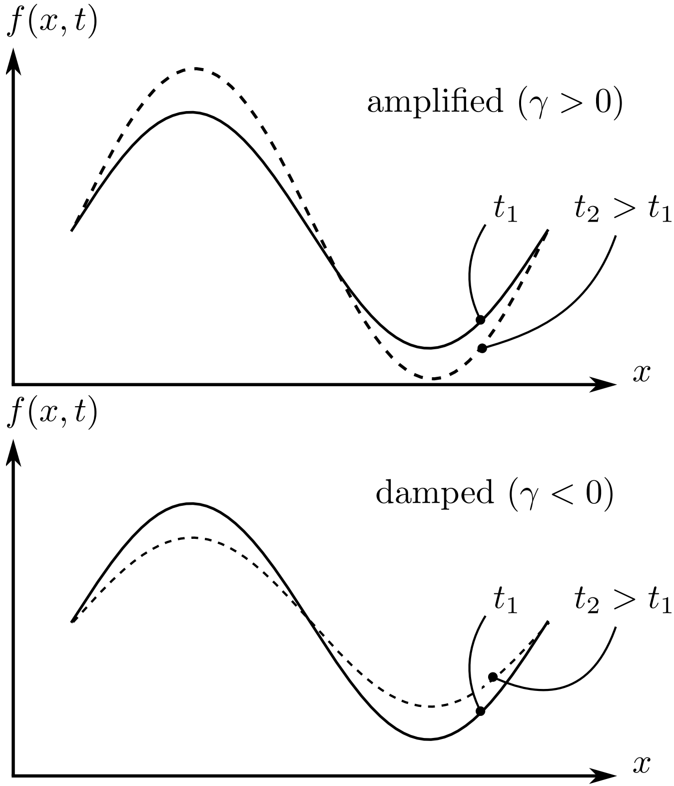

Figure 3: Sketch of aperiodic ($\omega_R = 0$) growing ($\gamma > 0$, top) and aperiodic damped ($\gamma < 0$, bottom) monochromatic fluctuation.

2. Fundamental cosmic ray astrophysics

2.1. Key observations

(O1) Individual detected particle energies reach up to several 10^{20} eV for hadrons and 10^{14} eV for electrons (positrons and negatrons) with power law energy distributions $N(E) \propto E^{-s}$ over wide energy ranges.
In the kinetic energy range $10^8 - 10^{11}$ eV/Nucleon, with the highest intensities, the hadron component consists of ~ 87 percent protons, ~ 12 percent α-particles and ~ 1 percent heavier nuclei from carbon to the actinides. Apart from positrons and antiprotons (from secondary productions) no antiparticles have been detected.

(O2) At relativistic energies there are about 100 times more hadrons then electrons.

(O3) The arrival directions of CRs are highly isotropic, although their sources are located in the galactic plane, so that an efficient scattering mechanism of the particles during their propagation from their sources to us is required!

(O4) Abundance measurements of the ^{10}Be-isotope at kinetic energies < 500 MeV/Nucleon indicate a mean age of nonrelativistic cosmic rays of about $< T > \simeq 10^7$ yrs. The size of our Galaxy $L \in [1, 30]$ kpc would imply a mean age of $2L/c \in [6000, 2 \cdot 10^5]$ yrs for free escape along the galactic magnetic field, at least two orders of magnitude too short. Again efficient scattering of the particles is required.

(O5) Measurements of CR secondary/primary ratios such as B/C indicate at relativistic energies for the traversed matter during galactic propagation

$$X_0 = c < n >< T > \simeq 7[E(20\,\mathrm{GeV/Nucleon})]^{-0.6}\ \mathrm{g\ cm}^{-2} \tag{3}$$

Obviously this requires a momentum-dependent mean age of CRs

$$< T > \simeq 10^7 [p(20\,\mathrm{GeV/cNucl.})]^{-0.6}\ \mathrm{yrs}, \tag{4}$$

implying a mean interstellar gas density of $< n > = 0.44$ cm^{-3}, smaller than typical gas density in galactic plane of $\simeq 1$ cm^{-3}. During their propagation CRs must have traversed the halo region and/or the dilute phases of the interstellar medium (ISM).

(O6) Time history studies of cosmogenic nuclei show that within a factor of 2 the flux of galactic CRs has been constant over the last 10^9 yrs.

(O7) Local observations (O1)-(O6) are by and large characteristic for the whole galaxy as the surveys of CR electron synchrotron radiation at radio frequencies and the diffuse high-energy gamma radiation from π^0-decay from hadronic production and electron production by bremsstrahlung and inverse Compton interactions indicate.

(O8) The sources of CRs (cosmic ray accelerators) reveal themselves by radiation products from interactions with ambient matter, radiation and magnetic fields: photons from electron interaction processes (synchrotron radiation, inverse Compton scattering, bremsstrahlung, pair annihilation) and hadron interaction processes (secondary pion production in inelastic hadron-hadron and hadron-photon collisions) with subsequent π^0-decay and secondary electron production from $\pi^{\pm}$-decays (also source of high-energy neutrinos).

Surveys of the FERMI gamma-ray satellite and the air-Cerenkov telescopes HESS, MAGIC and VERITAS (see lecture by C. Stegmann) and the ICECUBE neutrino telescope (see lecture by F. Halzen) have confirmed the "usual suspects" as CR sources: pulsar wind nebulae, supernova shock fronts, jets of active galactic nuclei and microquasars, which share a common feature: they are compact objects with high-velocity (often relativistic) outflows interacting with the ambient medium.

These observations tell us WHERE CRs are accelerated but not necessarily HOW they are accelerated! The fundamental crucial science question is: How is directed kinetic outflow energy converted into relativistic charged particles? The answer is provided by studying relativistic plasma beam physics!

Fig. 4 sketches the typical life of a CR particle: after being accelerated in individual sources such like supernova remnants, active galactic nuclei or gamma-ray bursts, it stochastically propagates in the partially turbulent magnetic field and interacts with the ambient photon and matter fields, generating nonthermal photon and neutrino radiation. In the case of galactic CRs this takes about 10^7 years before detection by near-Earth or ground based detectors.

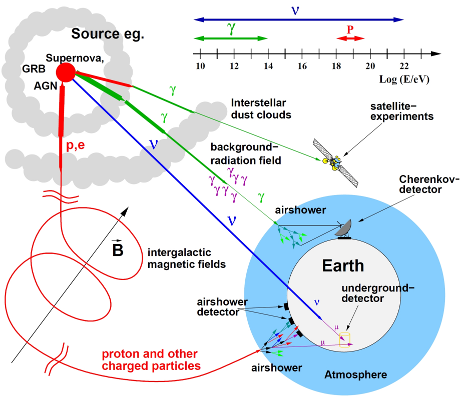

Figure 4: Sketch of cosmic ray life. Courtesy R. Wagner.

2.2. Immediate implications

The established relevant observations listed before allow us some immediate conclusions:

1) Using the observed isotropy (O3) we calculate the energy density

$$w = 4\pi \sum_i \int_0^\infty dE_{\mathrm{kin}} E_{\mathrm{kin}} N_i(E_{\mathrm{kin}}) = 0.5 \text{ eV cm}^{-3} = 0.8 \cdot 10^{-12} \text{ erg cm}^{-3} \tag{5}$$

and pressure $P = w/3 \simeq 3 \cdot 10^{-13}$ dyne cm^{-2} of cosmic ray hadrons by integrating the local energy distribution functions (O1) over all energies and summing over all species.
The CR energy density is comparable to the energy densities of the interstellar gas, the galactic magnetic field and the universal microwave background radiation which is referred to as the "global energy equipartition" in the ISM. Since today, this truly remarkable equipartition in the ISM has not been understood nor explained theoretically. Cosmic rays therefore play an important dynamical role in the Galaxy because of their comparable energy density and pressures with the other constituents, each of the order of 10^{-12} erg cm^{-3}.

2) The steady (O6) total (O7) luminosity of galactic CRs then is with the volume of galaxy $V \simeq 10^{67}$ cm^3, $T \simeq 3 \cdot 10^{14}$ s and 1 eV$= 1.6 \cdot 10^{-12}$ erg:

$$L = wV / < T > \simeq 10^{40} \text{erg s}^{-1}, \tag{6}$$

which has to be provided steadily by galactic sources and which restricts possible CR source clasees to supernova explosions, neutron stars and stellar winds from young hot O/B stars (the usual suspects).

3) The observed small degree of linear polarization of the synchrotron radiation from galactic CR electrons indicates that the galactic magnetic field contains a large turbulent component $\vec{B} = \vec{B}_0 + \delta\vec{B}$ with $|\delta\vec{B}| \simeq |\vec{B}_0|$.

4) The most likely scattering mechanism of CRs is pitch-angle scattering by the turbulent magnetic field fluctuations because of the lack of alternatives. Coulomb scatterings with the ISM particles are much too slow because of the low ISM gas density $< n >$.

5) The observed low electron/hadron ratio (O2) provides strong evidence for **electromagnetic** CR acceleration and transport processes in turbulent electromagnetic fields $\vec{B} = \vec{B}_0 + \delta\vec{B}$ and $\vec{E} = \vec{0} + \delta\vec{E}$.
No ordered large-scale electric field persists because of the huge ISM conductivity with two prominent exceptions: pulsar magnetospheres and transient magnetic reconnection phenomena.

CRs with total momentum p and charge q are subject to the Lorentz force:

$$\frac{d\vec{p}}{dt} = q\left[\delta\vec{E} + \frac{\vec{v}\times(\vec{B}_0 + \delta\vec{B})}{c}\right] \tag{7}$$

Any acceleration then requires turbulent electric fields because

$$\frac{dp^2}{dt} = 2\vec{p} \cdot \frac{d\vec{p}}{dt} = 2q\vec{p} \cdot \delta\vec{E} \tag{8}$$

One obtains equal acceleration rates for charged particles at the same magnetic rigidity $\vec{R} = \vec{p}/q$. Eq. (8) immediately provides for the rigidity

$$\frac{dR^2}{dt} = 2\vec{R} \cdot \delta\vec{E} \tag{9}$$

Consequently, any **electromagnetic acceleration process** orders particle distribution functions with respect to their rigidity.

2.3. Rigidity ordering

The rigidity ordering (9) explains the observed (O2) about 100 times more hadrons than electrons at relativistic energies $E_{\rm kin} \gg m_pc^2 = 1$ GeV because of the different proton and electron masses $m_p = 1836m_e$: we recall

$$E_{\rm kin} = \sqrt{p^2c^2 + m^2c^4} - mc^2,\ \ p = \frac{1}{c}\sqrt{E_{\rm kin}^2 + 2mc^2E_{\rm kin}} \tag{10}$$

Let us assume that electrons and protons are accelerated to the same power law spectrum for the differential number density $N_e(p) = N_{0,e}p_e^{-s}$, $N_p(p) = N_{0,p}p_p^{-s}$ in momentum(=rigidity here) above the same **nonrelativistic** kinetic energy $T_0 = 10$ keV, and have equal total number density $n_0 = \int_{p_e(T_0)}^{\infty} dp_e\, N_e(p_e)$ $= \int_{p_p(T_0)}^{\infty} dp_p\, N_p(p_p)$, implying

$$\frac{N_{0,e}}{N_{0,p}} = [\frac{p_p(T_0)}{p_e(T_0)}]^{1-s} \simeq (\frac{m_e}{m_p})^{\frac{s-1}{2}}, \tag{11}$$

as for $T_0 \ll m_e c^2 \ll m_p c^2$ Eq. (10) yields $p_e(T_0 \ll m_e c^2) \simeq \sqrt{2 m_e T_0}$ and $p_p(T_0 \ll m_p c^2) \simeq \sqrt{2 m_p T_0}$. With Eq. (10) we find

$$N(E_{\mathrm{kin}}) = N[p(E_{\mathrm{kin}})] \frac{dp}{dE_{\mathrm{kin}}} = \frac{N_0}{c}(E_{\mathrm{kin}} + mc^2) \left[\frac{E_{\mathrm{kin}}^2}{c^2} + 2E_{\mathrm{kin}} m\right]^{-(s+1)/2} \tag{12}$$

One obtains for the electron-proton ratio in the limit $T_0 \ll m_e c^2$

$$\frac{N_e(E_{\mathrm{kin}})}{N_p(E_{\mathrm{kin}})} = \left(\frac{m_e}{m_p}\right)^{(s-1)/2} \frac{E_{\mathrm{kin}} + m_e c^2}{E_{\mathrm{kin}} + m_p c^2} \left[\frac{E_{\mathrm{kin}} + 2m_e c^2}{E_{\mathrm{kin}} + 2m_p c^2}\right]^{-(s+1)/2}, \tag{13}$$

which at relativistic energies $E_{\mathrm{kin}} \gg m_p c^2$ =1 GeV approaches the constant

$$\frac{N_e(E_{\mathrm{kin}} \gg m_p c^2)}{N_p(E_{\mathrm{kin}} \gg m_p c^2)} \simeq \left(\frac{m_e}{m_p}\right)^{(s-1)/2} = 0.011 \tag{14}$$

for $s = 2.2$. Most electrons are distributed at nonrelativistic kinetic energies $T_0 \leq E_{\mathrm{kin}} \leq m_e c^2$. (This argument ignores the influence of momentum loss processes.)

2.4. Collision-free plasmas

All nonstellar cosmic plasmas are collision-free: plasma parameter $g = \nu_{ee}/\omega_{p,e} = \mathcal{O}\left(10^{-10}\right) \ll 1$, i.e. electromagnetic interactions dominate over elastic collisions. ν_{ee} denotes the electron-electron Coulomb collision frequency, $\omega_{p,e} = 5.64 \cdot 10^4 n_e^{1/2}$ Hz in CGS units characterizes the interactions of charged particles with electric fields.

Reasoning: Take typical time scale (τ) and length scale (l). The equation of motion (7) for nonrelativistic particle with $p = mv$ and $q = e$ in an electric field then reads

$$|\frac{d\vec{v}}{dt}| = |\frac{d^2\vec{x}}{dt^2}| \simeq \frac{l}{\tau^2} = |\frac{e}{m}\vec{E}| \simeq \frac{qE}{m} \tag{15}$$

The first Maxwell equation provides

$$|\mathrm{div}\,\vec{E}| \simeq \frac{E}{l} = |-4\pi e n_e|, \ \rightarrow E = 4\pi q n_e l \tag{16}$$

Inserting relation (16) into relation (15) yields

$$\frac{1}{\tau^2} = \frac{4\pi e^2 n_e}{m} = \omega_{p,e}^2 \frac{m_e}{m}, \ \ \omega_{p,e} = \sqrt{\frac{4\pi e^2 n_e}{m_e}}, \tag{17}$$

or $\tau = (m/m_e)\omega_{p,e}^{-1}$.

Likewise, with classical electron radius $r_e = e^2/m_e c^2 = 2.82 \cdot 10^{-13}$ cm

$$\nu_{ee} = \frac{4\pi e^4 n_e}{m_e^2 v_{\rm th}^3} = \omega_{p,e}^2 \frac{e^2}{m_e v_{\rm th}^3} = \omega_{p,e}^2 \frac{r_e m_e c^2}{m_e v_{\rm th}^3} = \frac{\omega_{p,e}^2 r_e}{c} (\frac{c}{v_{\rm th}})^3 = \frac{\omega_{p,e}^2 r_e}{c} [\frac{m_e c^2}{2k_B T}]^{3/2}, \tag{18}$$

providing for the plasma parameter

$$g = \frac{\nu_{ee}}{\omega_{p,e}} = \frac{\omega_{p,e} r_e}{c} [\frac{m_e c^2}{2k_B T}]^{3/2} = 8.7 \cdot 10^{-5} \frac{n_e^{1/2}}{T^{3/2}} \tag{19}$$

For the interstellar medium: $n_e = 1$ cm^{-3}, $T = 10^4$ K $\rightarrow$ $g = 8.7 \cdot 10^{-11}$.

Consequences:

- particle distribution functions are not Maxwellians resulting from dominance of elastic 2-body Coulomb collisions
- ideal MHD is not applicable
- if shock waves form, their properties are different from classical ideal MHD shocks
- full kinetic theory is required.

To a large extent, our progress in understanding CR dynamics in cosmic plasmas depends on our understanding of the magnetic and electric field fluctuations in collision-free plasmas.,

3. Basic kinetic equations

Because of the near energy equipartition between electromagnetic fields and particles, a fully complete description of their dynamics is necessary accounting for their various coupling and interaction processes.

3.1. Electromagnetic fields

The electromagnetic fields fulfill Maxwell equations

$$\nabla \times \vec{B}(\vec{x},t) - \frac{1}{c}\frac{\partial}{\partial t}\vec{E}(\vec{x},t) = \frac{4\pi}{c}\sum_a q_a \int d^3p\, \vec{v}\, N_a(\vec{x},\vec{p},t), \tag{20}$$

$$\nabla \cdot \vec{B}(\vec{x},t) = 0, \tag{21}$$

$$\nabla \times \vec{E}(\vec{x},t) + \frac{1}{c}\frac{\partial}{\partial t}\vec{B}(\vec{x},t) = 0. \tag{22}$$

$$\nabla \cdot \vec{E}(\vec{x},t) = 4\pi \sum_a q_a \int d^3p\, N_a(\vec{x},\vec{p},t), \tag{23}$$

where the charged particle's phase space distributions $N_a(\vec{x},\vec{p},t)$ determine the current and charge densities on the right-hand side of Eqs. (20) and (23).

3.2. Charged particles

Basic equations for the Klimontovich particle density of sort "a":

$$N_a(\vec{x},\vec{p},t) = \sum_{i=1}^{N_0} \delta[\vec{x}-\vec{x}_i(t)]\delta[\vec{p}-\vec{p}_i(t)],$$

$$\dot{\vec{x}}_i = \vec{v}_i = \frac{\vec{p}_i}{m_i\gamma_i}, \quad \dot{\vec{p}}_i = q_i[\vec{E}(\vec{x}_i,t) + \frac{\vec{v}_i \times \vec{B}(\vec{x}_i,t)}{c}] \tag{24}$$

The particle density (24) fulfils exactly Klimontovich equation for each species "a":

$$\frac{\partial N_a}{\partial t} + \vec{v}\cdot\frac{\partial N_a}{\partial \vec{x}} + q_a\left[\vec{E} + \frac{\vec{v}\times\vec{B}}{c}\right]\cdot\frac{\partial N_a}{\partial \vec{p}} = Q_a(\vec{x},\vec{p},t) \tag{25}$$

with the local electromagnetic fields $\vec{E}(\vec{x},t)$ and $\vec{B}(\vec{x},t)$.

These have to be determined from a solution of the Maxwell equations (20) - (23). The source term $Q_a(\vec{x},\vec{p},t)$ accounts for sources and sinks of particles and other (than the Lorentz force) electromagnetic interactions such as radiative reaction and/or the mirror force in nonuniform guide magnetic fields $\vec{B}_0$.

We immediately recognize the nonlinear couplings of the set of Eqs. (20)-(25): to determine the particle's phase space density from the Klimontovich equation we have to know the electromagnetic fields; but to determine the electromagnetic fields from Maxwell's equations we have to know the phase space density of the particles determining the charge and current densities. **We are facing the fundamental problem of plasma physics: the plasma particles determine the electromagnetic fields and vice versa in a highly nonlinear way.**

In order to proceed with a solution of this coupled problem two opposite points of view can be taken:

1) the *test fluctuations approach*, in which the plasma particle distribution functions are assumed to be given in a prescribed initial state, so that the resulting electromagnetic field and its properties can be calculated.

2) the *test particle approach*, in which the electromagnetic field is assumed to be given, so that the response of the particles can be calculated.

A consistent theory should combine these two approaches at least to a level of avoiding dramatic contradictions.

4. Cosmic gyrotropic particle distribution functions

Nonrelativistic Bi-Maxwellian:

$$F_a(v_\perp, v_\parallel) = \frac{1}{\pi^{3/2} v_{\mathrm{th,a,\perp}}^2 v_{\mathrm{th,a,\parallel}}} e^{-\frac{v_\perp^2}{v_{\mathrm{th,a,\perp}}^2} - \frac{v_\parallel^2}{v_{\mathrm{th,a,\parallel}}^2}} \tag{26}$$

Nonrelativistic isotropic Maxwellian ($v_{\mathrm{th,a,\perp}} = v_{\mathrm{th,a,\parallel}} = v_{\mathrm{th,a}}$):

$$F_a(v) = \frac{1}{\pi^{3/2} v_{\mathrm{th,a}}^3} e^{-\frac{v^2}{v_{\mathrm{th,a}}}} \tag{27}$$

Nonrelativistic Bi-Maxwellian with Strahl:

$$F_a(v_\perp, v_\parallel) = \frac{1}{\pi^{3/2} v_{\mathrm{th,a,\perp}}^2 v_{\mathrm{th,a,\parallel}}} e^{-\frac{v_\perp^2}{v_{\mathrm{th,a,\perp}}^2}} [e^{-\frac{(v_\parallel - V)^2}{v_{\mathrm{th,a,\parallel}}^2}} + e^{-\frac{(v_\parallel + V)^2}{v_{\mathrm{th,a,\parallel}}^2}}] \tag{28}$$

Nonrelativistic anisotropic Cairns-distribution (with nonthermality parameter $\alpha \geq 0$):

$$F_a(v_\perp, v_\parallel) =$$

$$\frac{1}{\pi^{3/2}(1+\frac{15\alpha}{4})v^2_{\mathrm{th,a,}\perp}v_{\mathrm{th,a,}\parallel}}[1+\alpha(\frac{v^2_\perp}{v^2_{\mathrm{th,a,}\perp}}+\frac{v^2_\parallel}{v^2_{\mathrm{th,a,}\parallel}})^2]e^{-\frac{v^2_\perp}{v^2_{\mathrm{th,a,}\perp}}-\frac{v^2_\parallel}{v^2_{\mathrm{th,a,}\parallel}}} \tag{29}$$

Nonrelativistic Bi-Kappa (Γ denotes gamma-function):

$$F_a(v_\perp, v_\parallel) = \frac{1}{\pi^{3/2}\Theta^2_{\mathrm{a,}\perp}\Theta_{\mathrm{a,}\parallel}}\frac{\Gamma(\kappa_a+1)}{\kappa_a^{3/2}\Gamma(\kappa_a-\frac{1}{2})}\left[1+\frac{v^2_\perp}{\kappa_a\Theta^2_{\mathrm{a,}\perp}}+\frac{v^2_\parallel}{\kappa_a\Theta^2_{\mathrm{a,}\parallel}}\right]^{-(\kappa_a+1)} \tag{30}$$

Nonrelativistic isotropic Kappa (Γ denotes gamma-function):

$$F_a(v) = \frac{1}{\pi^{3/2}\Theta^3_{\mathrm{a}}}\frac{\Gamma(\kappa_a+1)}{\kappa_a^{3/2}\Gamma(\kappa_a-\frac{1}{2})}\left[1+\frac{v^2}{\kappa_a\Theta^2_{\mathrm{a}}}\right]^{-(\kappa_a+1)} \tag{31}$$

All distribution functions normalized to $\int d^3v F_a = 1$.

Fig. 5 displays the isotropic Maxwellian and Kappa distribution functions. For $\kappa_a \to \infty$ the Kappa distribution function approaches the Maxwellian distribution function. The Kappa distribution function allows for suprathermal particles in its high-velocity tail (with power-law $\propto v^{-2(\kappa_a+1)}$) as often observed in space distribution functions.

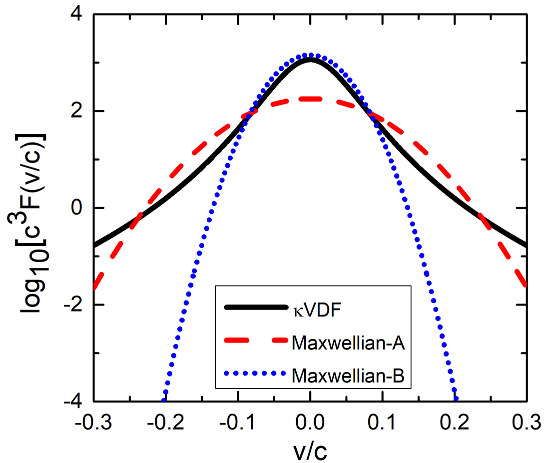

Figure 5: Isotropic nonrelativistic Maxwellian and Kappa distribution functions

5. In-situ observations of particle distribution functions and electromagnetic fluctuations

The solar wind plasma is the only cosmic plasma where detailed in-situ satellite observations of plasma properties are available (Bale et al. 2009). As other dilute cosmic plasmas have similar densities, temperatures and magnetic fields as the solar wind, the physical processes there probably are the same.

Fluctuations occur in all plasmas, including those in thermal equilibrium and unmagnetized plasmas, so that their state variables such as density, pressure and electromagnetic fields fluctuate in position and time. The study of electromagnetic fluctuations has a long history. The monographs of Sitenko (1967), Ichimaru (1973) and Kegel (1998) review the standard literature.

5.1. Interplanetary observations

Although the detailed plasma relaxation processes are not understood, the observed electron and proton distribution functions are close to the bi-Maxwellian velocity distribution (26) with different temperatures along and perpendicular to the ordered magnetic field direction, which are special cases of velocity-anisotropic particle distribution functions (VADs):

$$F_a(v_\perp, v_\parallel) \propto \exp\left[-\frac{mv_\parallel^2}{2k_BT_\parallel} - \frac{mv_\perp^2}{2k_BT_\perp}\right] \qquad (32)$$

Ten years (long-time average) of WIND/SWE data (see Fig. 6) have demonstrated that in the parameter plane, defined by the temperature anisotropy $A = T_\perp / T_\parallel$ and the parallel plasma beta $\beta_\parallel = 8\pi n_e k_B T_\parallel / B_0^2 = P_{\mathrm{thermal},\parallel} / P_B$, stable plasma configuration are only possible within a rhomb-like configuration around $\beta_\parallel \simeq 1$.

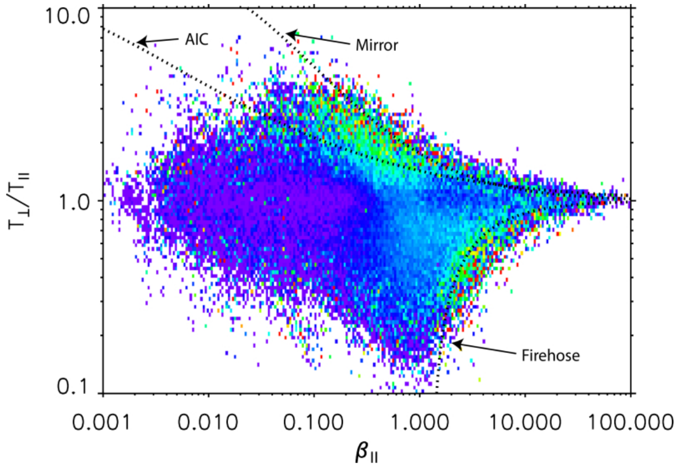

Figure 6: Magnitude of observed magnetic fluctuations $|\delta B|$ (from Bale et al. 2009)

At large values $\beta_{\|} \geq 1$ of the parallel plasma beta the boundararies of the rhomb coincide with the criteria for marginal instability of the **mirror and firehose fluctuations** (Hellinger et al. 2006), whereas at small plasma betas the boundaries of the rhomb are given by the criteria for marginal instability of the parallel propagating **Alfven waves** (RS and Skoda 2010) generated by the bi-Maxwellian proton and electron distributions.

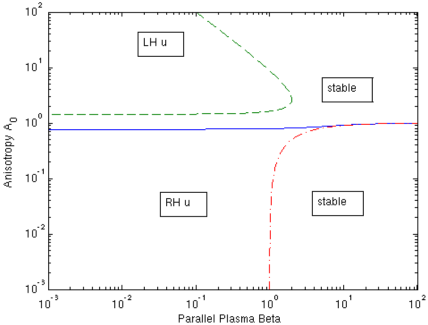

Figure 7: Anisotropy diagram of LH (dashed curve) and RH (full curve) polarized Alfven waves. Unstable regions are marked by "u". The dot-dashed curve illustrates the constaint $A_0 > 1 - \beta_{\|}^{-1}$.

The following likely explanation emerges: in the parameter plane defined by the temperature anisotropy $A = T_\perp/T_\parallel$ and the parallel plasma beta $\beta_\parallel$, stable plasma configuration are only possible within a rhomb-like configuration around $\beta_\parallel \simeq 1$, whose limits are defined by the threshold conditions for the mirror, firehose and Alfven instabilities. If a plasma would start with parameter values outside this rhomb-like configuration, it immediately would generate fluctuations via the mirror, firehose and Alfven instabilities, which quickly relax (Yoon 2007a) the plasma distribution into the stable regime within the rhomb-configuration. Within the rhomb-configuration the observed magnetic fluctuations are generated by spontaneous emission (Yoon 2007b, Tautz and RS 2007) of the stable particle distribution functions.

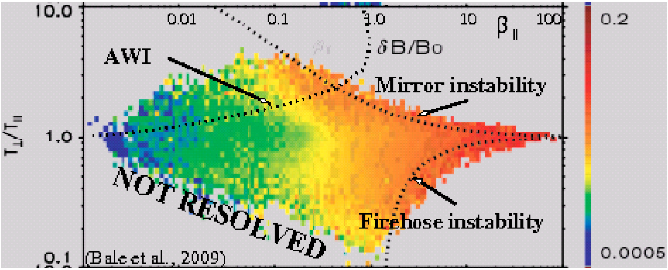

Figure 8: Comparison of marginal growth rate with observations of Bale et al. (2009).

5.2. Observed wavenumber spectra from single spacecraft in solar wind

The time-Fourier analysis of the observed fluctuations $(\delta B)^2(t)$ by a single spacecraft provides the frequeny spectrum $(\delta B)^2(f_{\mathrm{observed}})$ (see Fig. 9).

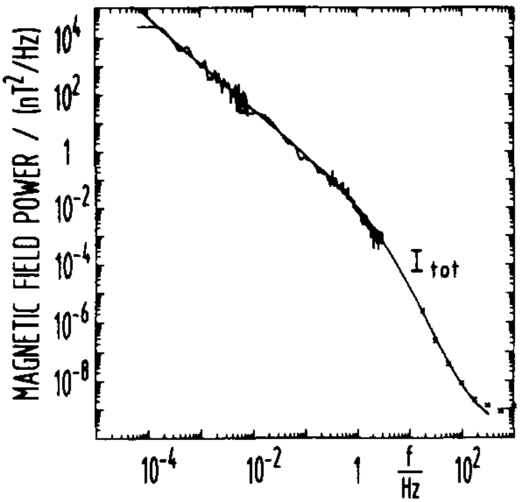

Figure 9: Solar wind transverse magnetic field turbulence frequency spectrum observed by ISEE 3 on 7 June 1980.

With

$$f_{\text{observed}} = f + \frac{\vec{V}_{\text{SW}} \cdot \vec{k}}{2\pi} \simeq \frac{k V_{\text{SW}} \cos\psi}{2\pi}, \tag{33}$$

where $\psi = \angle(\vec{k}, \vec{V}_{rmSW})$ one derives the wavenumber spectrum

$$(\delta B)^2(k) \propto (\delta B)^2 \left(\frac{2\pi f_{\text{observed}}}{V_{\text{SW}} \cos\psi} \right) \tag{34}$$

At low frequencies $f < 1 \simeq \Omega_p/2\pi$ Hz (in the so-called inertial range) one often finds Kolmogorov-type specta $(\delta B)^2(k) \propto k^{-5/3}$, while in the so-called dissipation range $f > 1$ Hz the spectrum considerably steepens.

6. Decoupling of cosmic ray from fluctuation dynamics

Fig. 10 shows the observed kinetic energy distribution functions of protons in the local interstellar medium. One distinguishes between

- Thermal protons at $E \simeq 10^{-6}$ MeV.
- Suprathermal protons 10^{-6} MeV $< E \leq 1$ MeV. Only constrained at $E > 13.6$ eV by the ionization and heating rate of the interstellar gas.
- Cosmic ray protons $E > 1$ MeV as observed by Voyager I.

Are these 3 different distinct distributions?
Or are these just different energy ranges of one common Kappa-distribution function?

Decoupling: in the first case one may treat the CRs as test particles in the stochastic electromagnetic fluctuations generated by thermal and/or suprathermal particles.

Fully coupled: in the second case a fully self-consistent analysis of the nonlinear plasma problem is required.

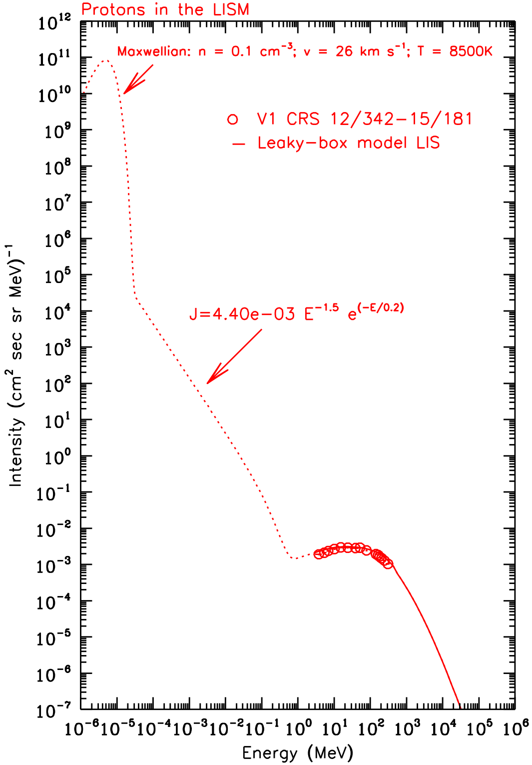

Figure 10: Protons in the local interstellar medium. From Cummings et al. (2016, ApJ 831, 18).

7. Summary

- We have reviewed the fundamentals of cosmic ray astrophysics stressing the importance of electromagnetic acceleration and transport processes with $B_0 \gg \delta B \gg \delta E$.
- Understanding cosmic $(\delta B, \delta E)$-fluctuations in magnetized plasmas is of crucial importance e.g. the role of collective and noncollective modes and wave-like and weakly-propagating fluctuations.
- We also reviewed the known in-situ observations of cosmic fluctuations and energetic charged particles.
- Financial support by the Deutsche Forschungsgemeinschaft and the Alexander-von-Humboldt-Stiftung is gratefully acknowledged.